

# Damped $\sin(\beta - \alpha)$ of Higgs couplings and the lightest Higgs production at $\gamma\gamma$ colliders in MSSM

Chao-Shang Huang<sup>\*</sup> and Xiao-Hong Wu<sup>†</sup>

Institute of Theoretical Physics, Chinese Academy of Sciences,  
P. O. Box 2735, Beijing 100080, P. R. China

## Abstract

In the decoupling limit,  $M_{A^0}^2 \gg M_Z^2$ , the heavy CP-even, CP-odd and charged Higgs boson masses are nearly degenerate,  $\sin(\beta - \alpha)$  approaches 1, and the lightest CP-even Higgs boson almost displays the same properties as the Standard Model Higgs boson. But the stop and sbottom sector can change this pattern through radiative corrections. We find that there are parameter regions at small, moderate and large  $\tan\beta$  in MSSM under experimental constraints of  $(g - 2)_\mu$  and  $b \rightarrow s\gamma$ , where  $\sin^2(\beta - \alpha)$  is damped (say below 0.8), which has a significant effect on Higgs couplings  $g_{h^0 VV}$  ( $V = W^\pm, Z^0$ ) and  $g_{h^0 \gamma\gamma}$ . We discuss its impact on the lightest CP-even Higgs production at  $\gamma\gamma$  colliders.

---

<sup>\*</sup>E-mail: csh@itp.ac.cn

<sup>†</sup>E-mail: wuxh@itp.ac.cn

## I. Introduction

The search for Higgs bosons and measurement of their properties are one of the most important tasks at present and future colliders. The Minimal Supersymmetry Standard Model(MSSM) has five physical Higgs bosons, two CP-even Higgs  $h^0$  and  $H^0$ , a CP-odd Higgs  $A^0$  and a charged Higgs pair  $(H^+, H^-)$  [1]. At tree level, the entire Higgs mass spectra and mixing angle  $\alpha$  of CP-even Higgs are determined by only two independent parameters, conveniently chosen CP-odd Higgs mass  $M_{A^0}$  and the ratio of two vacuum expectation values  $\tan\beta$ . And there is an upper bound on the mass of lightest CP-even Higgs  $h^0$ ,  $M_{h^0} < M_Z$ . However, radiative corrections can change this bound. At one loop level,  $M_{h^0}^2$  receives the  $G_F M_t^4$  term enhancement, which shifts  $M_{h^0}^{max}$  to 130GeV [2].

In the limit  $M_{A^0}^2 \gg M_Z^2$  (for  $M_{A^0} \geq 300\text{GeV}$ ), the charged, heavy CP-even and CP-odd Higgs bosons are nearly mass degenerate,  $M_{H^\pm} \simeq M_{H^0} \simeq M_{A^0}$ ,  $\sin(\beta-\alpha)$  approaches 1, and the properties of the lightest CP-even Higgs boson  $h^0$  are almost identical to those of the Standard Model (SM) Higgs boson  $h^{sm}$ . This is known as the decoupling limit [3]. When  $M_{A^0}$  is not too large, i.e., far from the decoupling limit,  $h^0$  and  $H^0$  mix severely and  $\sin(\beta-\alpha)$  is lifted from 1 [4].

Recently, the study of Higgs boson productions at photon colliders has been extensively carried out [5]. Photon colliders have distinct advantages in searches for and measurements of neutral Higgs bosons. At  $\gamma\gamma$  colliders, the Higgs boson can be produced in  $s$ -channel resonance, via triangle loop with all the charged particles which gives the unique opportunity to precisely measure the properties of Higgs boson, mass, production and decay channel and determine CP property and spin, parity [6]. And  $\gamma\gamma$  colliders give a chance to produce single heavy Higgs  $H^0$ ,  $A^0$ , which extends the mass reach. Compared with  $e^+e^-$  colliders, the heavy Higgs bosons are produced in pair, because the  $ZH^0$ ,  $ZA^0$  channels are suppressed due to nearly zero  $\cos(\beta-\alpha)$ . A simulation study of the production of the lightest Higgs boson and discovery potential at  $\gamma\gamma$  colliders has been given [7].

To study the Higgs boson productions at photon colliders is essentially to examine the loop induced coupling of Higgs bosons to photons  $g_{h^0\gamma\gamma}$ . The coupling  $g_{h^0\gamma\gamma}$  had been discussed long ago [8], recent revisit in the decoupling limit in MSSM as well as the tow-photon decay of the SM-like Higgs boson at photon colliders has been worked out [9]. Related with the decoupling limit, a question arises naturally. That is, is there any region with  $M_{A^0}^2 \gg M_Z^2$  of the parameter space in MSSM where the decoupling limit can be relaxed ( i.e., there are significant mass differences among  $M_{H^\pm}$ ,  $M_{H^0}$  and  $M_{A^0}$  and  $\sin(\beta - \alpha)$  deviates from 1 although  $M_{A^0}^2 \gg M_Z^2$  )? In this paper we would like to answer the question and discuss its phenomenological implication on the light neutral Higgs boson production at photon colliders. It is shown that the decoupling limit can be relaxed in some regions with  $M_{A^0}^2 \gg M_Z^2$  of the parameter space which are allowed by experiments of  $(g - 2)_\mu$ ,  $b \rightarrow s\gamma$  and lower bounds of sparticle masses, due to the large off-diagonal scalar top and scalar bottom mass matrix elements contributing to the Higgs sector by radiative corrections. In the regions, the charged, heavy CP-even and CP-odd Higgs bosons are not mass degenerate, and  $\sin^2(\beta - \alpha)$  can be damped (say, below 0.8) from 1, the value in the decoupling limit, which has significant effect to the couplings proportional to  $\sin(\beta - \alpha)$ , most importantly  $g_{h^0VV}$ , ( $V = W^\pm, Z$ ) and consequently  $g_{h^0\gamma\gamma}$  (note that the dominant contribution to  $g_{h^0\gamma\gamma}$  comes from  $W^+W^-$  loop, which is proportional to  $g_{h^0W^+W^-}$ ). The discovery potential of Higgs bosons in experiments relies heavily on these couplings.

The paper is organized as follows. In section II we analyze how the decoupling limit can be relaxed when including the radiative corrections to the neutral Higgs boson mass matrix. The experimental constraints on the parameter space in MSSM are discussed in section III and the formula concerned with the light neutral Higgs boson production at photon coliders are listed in section IV. We present our numerical results in section V. Finally, in section VI we end up with concluding remarks.

## II. CP-even Higgs mass matrix and $\sin^2(\beta - \alpha)$

The mass-squared matrix of two CP-even Higgs bosons  $h^0$  and  $H^0$  is given by

$$M_{\mathcal{H}}^2 = \begin{pmatrix} M_{11}^2 & M_{12}^2 \\ M_{12}^2 & M_{22}^2 \end{pmatrix} = \begin{pmatrix} M_{A^0}^2 s_\beta^2 + M_Z^2 c_\beta^2 + \delta M_{11}^2 & -(M_{A^0}^2 + M_Z^2) s_\beta c_\beta + \delta M_{12}^2 \\ -(M_{A^0}^2 + M_Z^2) s_\beta c_\beta + \delta M_{12}^2 & M_{A^0}^2 c_\beta^2 + M_Z^2 s_\beta^2 + \delta M_{22}^2 \end{pmatrix} \quad (1)$$

$c_\beta, s_\beta$  denote  $\cos \beta$  and  $\sin \beta$ .  $\delta M_{ij}^2 (i, j = 1, 2)$  are generated through radiative corrections from loops of fermions and sfermions and proportional to the fermion Yukawa couplings squared. The dominant contribution comes from the the third generation, which has large fermion masses. The corresponding top and bottom squark mass-squared matrix in  $(\tilde{q}_L, \tilde{q}_R)$  basis are expressed in MSSM as

$$M_{\tilde{t}}^2 = \begin{pmatrix} M_{\tilde{q}}^2 + M_t^2 + (\frac{1}{2} - \frac{2}{3} \sin^2 \theta_W) M_Z^2 \cos 2\beta & M_t(A_t - \mu \cot \beta) \\ M_t(A_t - \mu \cot \beta) & M_{\tilde{t}_R}^2 + M_t^2 + \frac{2}{3} \sin^2 \theta_W M_Z^2 \cos 2\beta \end{pmatrix} \quad (2)$$

$$M_{\tilde{b}}^2 = \begin{pmatrix} M_{\tilde{q}}^2 + M_b^2 + (-\frac{1}{2} + \frac{1}{3} \sin^2 \theta_W) M_Z^2 \cos 2\beta & M_b(A_b - \mu \tan \beta) \\ M_b(A_b - \mu \tan \beta) & M_{\tilde{b}_R}^2 + M_b^2 - \frac{1}{3} \sin^2 \theta_W M_Z^2 \cos 2\beta \end{pmatrix} \quad (3)$$

The radiative corrections to  $\delta M_{ij}^2 (i, j = 1, 2)$ , including dominant one-loop top, bottom quark and top, bottom squark corrections and two-loop leading logarithmic contributions are given in [10]. In our numerical calculation we used the results of radiative corrections to the CP-even Higgs mass matrix based on ref. [11] that incorporates the one-loop effective potential and two-loop leading-log contribution from arbitrary off-diagonal stop and sbottom matrices. In the limit of vanishing off-diagonal parameters  $\mu$ ,  $A_t$  and  $A_b$ ,  $\delta M_{11}^2$  and  $\delta M_{12}^2$  is 0, and  $\delta M_{22}^2 = \frac{3g^2}{8\pi^2 M_W^2} \frac{M_t^4}{\sin^2 \beta} \ln(1 + \frac{M_{\tilde{q}}^2}{M_t^2})$ , which lifts the upper bound of lightest Higgs mass  $M_{h^0}$  above  $M_Z$  [2].

The neutral CP-even Higgs mass eigenvalues can be derived from Eq. (1) as

$$M_{h^0, H^0} = \frac{\text{Tr} M_{\mathcal{H}}^2 \mp \sqrt{(\text{Tr} M_{\mathcal{H}}^2)^2 - 4 \det M_{\mathcal{H}}^2}}{2} \quad (4)$$

where  $Tr M_{\mathcal{H}}^2 = M_{11}^2 + M_{22}^2$ ,  $\det M_{\mathcal{H}}^2 = M_{11}^2 M_{22}^2 - (M_{12}^2)^2$ .

The mixing angle  $\alpha$  of CP-even Higgs bosons can be defined as

$$\tan 2\alpha = \frac{\sin 2\beta(M_{A^0}^2 + M_Z^2) - 2\delta M_{12}^2}{\cos 2\beta(M_{A^0}^2 + M_Z^2) + \delta M_{22}^2 - \delta M_{11}^2} \quad \left(-\frac{\pi}{2} < \alpha < \frac{\pi}{2}\right) \quad (5)$$

In the decoupling limit, all  $\delta M_{ij}^2 (i, j = 1, 2)$  are order of  $M_Z^2$  or smaller than that, then  $\alpha \sim \beta - \frac{\pi}{2}$ , and  $\sin(\beta - \alpha) \sim 1$ . However,  $\sin(\beta - \alpha)$  can deviate from 1 in some cases. In order to see this explicitly, let us look at the cases of moderate and large  $\tan \beta$ . For moderate and large  $\tan \beta$  (say,  $\tan \beta = 10$ ),  $\cos 2\beta \simeq -1$  and  $\sin 2\beta \simeq 2 \cot \beta$ . Then, when the numerator is not too small (of order  $M_Z^2$ ), and the large  $-M_{A^0}^2$  term in the denominator of Eq. (5) is compensated by the radiative correction  $\delta M_{11}^2$  or  $\delta M_{22}^2$  or both,  $\alpha$  will largely deviates from  $\beta - \frac{\pi}{2}$  (e.g.,  $\alpha \sim 0.5$ ) and consequently  $\sin(\beta - \alpha)$  can be lifted from 1.

### III. Experimental constraints of $(g - 2)_\mu$ and $b \rightarrow s\gamma$

In this section we analyze the experimental constraints from  $(g - 2)_\mu$  and  $b \rightarrow s\gamma$  which will be imposed on the parameter space of MSSM in our numerical analysis.

The muon anomalous magnetic moment  $a_\mu \equiv \frac{1}{2}(g - 2)_\mu$  constraint from the recent Brookhaven E821 experiment [12] gives a  $2\sigma$  bound on the supersymmetry contribution,

$$11 \times 10^{-10} < a_\mu^{SUSY} < 75 \times 10^{-10}. \quad (6)$$

The one loop supersymmetric contributions to  $a_\mu$  come from the diagrams with chargino-sneutrino in the loop and neutralino-smuon in the loop respectively [13]. The chargino contribution is given in the limit of  $|M_2| \ll |\mu|$ ,

$$\delta a_\mu^{\tilde{\chi}^\pm} = 1.5 \tan \beta \left(\frac{200\text{GeV}}{M_{\tilde{\nu}}}\right)^2 \left(\frac{M_2}{100\text{GeV}}\right) \left(\frac{1000\text{GeV}}{\mu}\right) \left(\frac{F_2^C(\frac{M_2^2}{M_{\tilde{\nu}}^2})}{3}\right) 10^{-10}, \quad (7)$$

where  $F_2^C(x)$  is defined in [13], with  $F_2^C(1) = 1$ ,  $F_2^C(0.25) = 2.5$ . When  $\tan \beta$  is large, it can contribute within the experimental bound. The neutralino contribution can be important

from Bino- smuon loop, as emphasized by Martin and Wells in ref. [13]. In the large  $\mu$  (say  $\mu \sim 1\text{TeV}$ ) limit,  $|M_1| \ll |M_2|, |\mu|$  and two smuon are nearly degenerate  $m_{\tilde{\mu}_1} \simeq m_{\tilde{\mu}_2}$ . The Bino contribution can be written as

$$\delta a_\mu^{\text{B-ino}} = 3.0 \tan \beta \left( \frac{M_1}{100\text{GeV}} \right) \left( \frac{\mu - A_\mu \cot \beta}{1000\text{GeV}} \right) \left( \frac{200\text{GeV}}{M_{\tilde{\mu}}} \right)^4 \left( \frac{F_2^{N'}(\frac{M_\mu^2}{M_{\tilde{\mu}}^2})}{3} \right) 10^{-10} \quad (8)$$

where  $F_2^{N'}(x)$  is defined as  $F_2^{N'}(x) = 2F_2^N(x) + 2xdF_2^N(x)/dx$ , with  $F_2^{N'}(1) = 1$  and  $F_2^{N'}(0.25) = 2.4$ . The  $(\mu - A_\mu \cot \beta) \tan \beta$  term in Eq. (8) comes from smuon mixing. It is obvious that when  $\mu \tan \beta$  is large (say,  $\mu \tan \beta \sim 20\text{TeV}$ ) and  $M_{\tilde{\mu}}$  is not too large, the experimental constraint of  $(g-2)_\mu$  can be satisfied by the Bino contribution.

The  $b \rightarrow s\gamma$  decay branch ratio from CLEO [14] is given as

$$2 \times 10^{-4} < BR_{exp}(b \rightarrow s\gamma) < 4.2 \times 10^{-4}. \quad (9)$$

In our numerical analysis, we use the leading order calculation of  $BR(b \rightarrow s\gamma)$  because of the lack of full next-to-leading order calculations in MSSM, and additional  $\pm 30\%$  uncertainty of the leading order calculation of  $b \rightarrow s\gamma$  has been considered. In this paper, since  $M_{H^\pm}$  ( $M_{H^\pm} \sim 300\text{GeV}$ ) is not too large, it can enhance the  $BR(b \rightarrow s\gamma)$  significantly because of the constructive contributions of the charged Higgs  $H^\pm$  and Standard Model (SM) charged gauge boson  $W^\pm$ . This gives a serious constraint on the supersymmetric contributions such that they must be destructively interferent with those in SM. In supergravity models with large  $\tan \beta$ , the chargino contribution is correlated to the sign of the product of  $\mu$  and  $A_t$ . For positive  $\mu A_t$ , the chargino contribution interferes with that in SM constructively, and for negative  $\mu A_t$ , destructively [15].

#### IV. The Lightest Higgs boson production at $\gamma\gamma$ colliders

We follow the formula given in [9] [16]. The  $\gamma\gamma$  width of the lightest Higgs is expressed as

$$\Gamma(h \rightarrow \gamma\gamma) = \frac{\alpha^2 g_2^2}{1024\pi^3} \frac{m_h^3}{M_w^2} \left| \sum_i I_h^i \right|^2 \quad (10)$$

where  $i$  runs over all the loop contributions. The different kinds of  $I_h^i$  are given as

$$I_h^f = N_{cf} Q_f^2 R_f F_{1/2}(\tau_f), \quad (11)$$

$$I_h^w = R_w F_1(\tau_w), \quad (12)$$

$$I_h^{H^\pm} = R_{H^\pm} \frac{M_W^2}{M_{H^\pm}^2} F_0(\tau_{H^\pm}), \quad (13)$$

$$I_h^{\tilde{f}} = N_{cf} Q_f^2 R_{\tilde{f}} \frac{M_Z^2}{M_{\tilde{f}}^2} F_0(\tau_{\tilde{f}}), \quad (14)$$

$$I_h^{\chi^\pm} = R_{\chi^\pm} \frac{M_W}{M_{\chi^\pm}} F_{1/2}(\tau_{\chi^\pm}) \quad (15)$$

where  $\tau_i = 4M_i^2/M_h^2$ ,  $N_c = 3$  for quarks and squarks,  $N_c = 1$  for leptons and sleptons, the loop functions  $F_{1/2}(x)$ ,  $F_1(x)$ ,  $F_0(x)$  are given in Ref. [9] [16], and  $R_i$  are defined as follow

$$R_{u,c,t} = \frac{\cos \alpha}{\sin \beta}, \quad (16)$$

$$R_{d,s,b,e,\mu,\tau} = -\frac{\sin \alpha}{\cos \beta}, \quad (17)$$

$$R_W = \sin(\beta - \alpha), \quad (18)$$

$$R_{H^\pm} = \sin(\beta - \alpha) + \frac{\cos 2\beta \sin(\beta + \alpha)}{2 \cos^2 \theta_W}, \quad (19)$$

$$R_{\tilde{f}_{L,R}} = \frac{M_f^2}{M_Z^2} R_f \mp (I_f^3 - Q_f \sin^2 \theta_W) \sin(\beta + \alpha), \quad (20)$$

$$R_{\chi_i^\pm} = 2(S_{ii} \cos \alpha - Q_{ii} \sin \alpha) \quad (21)$$

If  $\tan \beta$  is large, the bottom Yukawa coupling receives the large correction, the coupling  $R_b$  is

$$R_b \simeq -\frac{\sin \alpha}{\cos \beta} \frac{1}{1 + \Delta_b} \left(1 - \frac{\Delta_b}{\tan \alpha \tan \beta}\right). \quad (22)$$

In Eq. (22)  $\Delta_b$  is given at one-loop as [17]

$$\Delta_b \simeq \frac{2\alpha_s}{3\pi} M_{\tilde{g}} \mu \tan \beta I(M_{\tilde{b}_1}, M_{\tilde{b}_2}, M_{\tilde{g}}) + \frac{Y_t}{4\pi} A_t \mu \tan \beta I(M_{\tilde{t}_1}, M_{\tilde{t}_2}, \mu) \quad (23)$$

where  $\alpha_s = g_s^2/4\pi$  and  $Y_t = h_t^2/4\pi$ ,  $h_t$  is top Yukawa coupling and the function  $I$  is defined by

$$I(x, y, z) = \frac{x^2 y^2 \ln(x^2/y^2) + y^2 z^2 \ln(y^2/z^2) + z^2 x^2 \ln(z^2/x^2)}{(x^2 - y^2)(y^2 - z^2)(x^2 - z^2)} \quad (24)$$

Since the off-diagonal elements of the mass-squared matrix of the third generation sfermion are large, which is considered in this paper, left- and right-handed sfermion mixing should be included in the Higgs sfermion couplings. In stead of Eq. (20), one has

$$R_{\tilde{f}_1} = \frac{M_f^2}{M_Z^2} R_f - (I_f^3 \cos^2 \theta_{\tilde{f}} - Q_f \sin^2 \theta_w \cos 2\theta_{\tilde{f}}) \sin(\beta + \alpha) - \frac{M_f \sin 2\theta_{\tilde{f}}}{2M_Z^2 \sin \beta} (A_f \cos \alpha - \mu \sin \alpha), \quad (25)$$

$$R_{\tilde{f}_2} = \frac{M_f^2}{M_Z^2} R_f - (I_f^3 \sin^2 \theta_{\tilde{f}} + Q_f \sin^2 \theta_w \cos 2\theta_{\tilde{f}}) \sin(\beta + \alpha) + \frac{M_f \sin 2\theta_{\tilde{f}}}{2M_Z^2 \sin \beta} (A_f \cos \alpha - \mu \sin \alpha) \quad (26)$$

for the top squark and

$$R_{\tilde{f}_1} = \frac{M_f^2}{M_Z^2} R_f - (I_f^3 \cos^2 \theta_{\tilde{f}} - Q_f \sin^2 \theta_w \cos 2\theta_{\tilde{f}}) \sin(\beta + \alpha) - \frac{M_f \sin 2\theta_{\tilde{f}}}{2M_Z^2 \sin \beta} (A_f \sin \alpha - \mu \cos \alpha), \quad (27)$$

$$R_{\tilde{f}_2} = \frac{M_f^2}{M_Z^2} R_f - (I_f^3 \sin^2 \theta_{\tilde{f}} + Q_f \sin^2 \theta_w \cos 2\theta_{\tilde{f}}) \sin(\beta + \alpha) + \frac{M_f \sin 2\theta_{\tilde{f}}}{2M_Z^2 \sin \beta} (A_f \sin \alpha - \mu \cos \alpha) \quad (28)$$

for the bottom squark and tau slepton, where  $\theta_{\tilde{f}}$  is the sfermion mixing angle.

The production cross section of the lightest Higgs boson at  $\gamma\gamma$  colliders is given as

$$\begin{aligned} \sigma(\gamma\gamma \rightarrow h) &= \frac{8\pi^2}{M_h^3} \Gamma(h \rightarrow \gamma\gamma) \delta(1 - \frac{\sqrt{s}}{M_h^2}) \\ &= \sigma_0 \delta(1 - \frac{\sqrt{s}}{M_h^2}) \end{aligned} \quad (29)$$

with

$$\sigma_0 = \frac{8\pi^2}{M_h^3} \Gamma(h \rightarrow \gamma\gamma) \quad (30)$$

where  $\sqrt{s}$  is the energy of mass center.

## V. Numerical analyses

In our numerical work, for simplicity, we assume the universal soft supersymmetry breaking squark mass  $M_{\tilde{q}} = M_{\tilde{t}_R} = M_{\tilde{b}_R} = M_{\tilde{c}_R} = M_{\tilde{s}_R} = M_{\tilde{u}_R} = M_{\tilde{d}_R}$ , and universal soft supersymmetry breaking slepton mass  $M_{\tilde{l}} = M_{\tilde{\tau}_R} = M_{\tilde{\mu}_R}$  which is different from the squark sector. With the assumption of the universal slepton mass, the requirement that the stau mass should be positive



puts a severe constraint on smuon mass matrix elements, because the only difference between the stau and smuon mass matrices is just that  $M_\tau$  in the stau mass matrix is replaced by  $M_\mu$  in the smuon mass matrix. With  $M_{\tilde{l}}^2 > M_\tau \tan \beta |\mu - A_\tau \cot \beta|$  and  $M_\tau/M_\mu \simeq 17$ , the two smuon mass are nearly degenerate, but smuon mixing angle is nonzero in the limit of large  $\mu \tan \beta$ . We analyze the parameter region under experimental constraints from lower bounds of supersymmetry particles and Higgs bosons [18],  $b \rightarrow s\gamma$  and the muon anomalous magnetic moment ( $g - 2$ ) in three cases: (a) low  $\tan \beta$ , (b) moderate  $\tan \beta$ , (c) large  $\tan \beta$ . In all our analyses and numerical work, we take  $A_\mu = A_\tau = 0$ , because of large  $\mu \tan \beta$  in the off-diagonal mass matrix elements ( $A_{\mu,\tau} - \mu \tan \beta$ ). We also fix  $M_{\tilde{g}} = 1\text{TeV}$ . This parameter only appears in the bottom Yukawa correction  $\Delta_b$ . The radiative corrections to the CP-even Higgs mass matrix element  $\delta M_{ij}^2 (i, j = 1, 2)$  depend on top and bottom squark mass matrix parameters  $M_{\tilde{q}}, \mu, A_t$  and  $A_b$ . The neutralino as the lightest supersymmetry particle (LSP) is also assumed.

First, we work in the small  $\tan \beta$  case, say  $\tan \beta = 4$ . Compared with the top Yukawa coupling, the bottom Yukawa coupling is small, and  $A_b = 0$  is taken. We fix  $M_{\tilde{q}}, M_{\tilde{l}}, M_{A^0}, A_b, M_1$  and  $M_2$ , all the triangle, star and dotted areas shown in Fig. 1 are experimentally allowed. In this parameter region,  $M_1 = 100\text{GeV}$  and  $M_2 = 450\text{GeV}$ , the dominant contribution to the muon anomalous magnetic moment ( $g - 2$ ) comes from the neutralino-smuon loop. In the region,  $\mu \sim 5\text{TeV}$ , the chargino-sneutrino loop contribution is negligible as it can be seen from Eq. (7). Because of large chargino and stop masses and low  $\tan \beta$ , the  $b \rightarrow s\gamma$  can be satisfied easily. When we further require  $\sin^2(\beta - \alpha) \leq 0.8$ , the two regions denoted by triangle and star appear, corresponding to the CP-even Higgs mixing angle  $\alpha > 0$  and  $\alpha < 0$  respectively. We see that in the two regions  $\mu$  is in the range between  $9.3M_{\tilde{q}}$  and  $10M_{\tilde{q}}$  and  $A_t$  is within a small range near 0. When  $M_{A^0}$  is raised, the allowed parameter region is decreased, as can be seen by comparing the Fig. 1A and 1B. As an illustration, we present two points in Fig. 1A as the cases A and B in Tab. I, corresponding to the positive and negative CP-even Higgs mixing angle  $\alpha$  respectively. We can see  $\sqrt{|\delta M_{22}^2|}$  and  $\sqrt{|\delta M_{12}^2|}$  are the same order as  $M_Z$ , but  $\delta M_{11}^2$  is

about a factor of 6 increase of  $\delta M_{22}^2$  in magnitude. With  $\cos 2\beta \simeq -0.6$ ,  $\sin 2\beta \simeq 2 \cot \beta \simeq 0.4$ , we notice that in the denominator of Eq. (5), the  $M_{A^0}^2$  term and  $\delta M_{11}^2$  term compensate each other with an order of magnitude larger than the numerator. This fine-tune gives the value of  $|\alpha| \sim 0.75$ , and reduces  $\sin^2(\beta - \alpha)$ . With this picture in mind, we can understand that when  $M_{A^0}$  increases, the fine-tune of  $M_{A^0}^2$  and  $\delta M_{11}^2$  terms in the denominator of Eq. (5) becomes more difficult, and as shown Fig. 1B, we get a parameter region significantly smaller than that in Fig. 1A.

Second, in the case of moderate  $\tan \beta = 10$ , we fix  $M_{\tilde{q}}$ ,  $M_{\tilde{l}}$ ,  $M_{A^0}$ ,  $A_b$ ,  $M_1$  and  $M_2$ , and the experimentally allowed area is denoted by the dotted and star areas as shown in Fig. 2. In this parameter region, because  $\mu \simeq 3\text{TeV}$  and  $\tan \beta = 10$ , the chargino contribution to the muon anomalous magnetic moment ( $g - 2$ ) is not large enough to rest in the experimental bound. The dominant contribution to  $a_\mu$  comes from the neutralino- sneutrino loop as seen from Eq. (8). In Fig. 2 the star area corresponds to the region of the parameter space where  $\sin^2(\beta - \alpha) \leq 0.8$ . We see that  $\mu$  is in the range between  $4.8M_{\tilde{q}}$  and  $7.3M_{\tilde{q}}$  and  $A_t$  is in a small range near  $3.5M_{\tilde{q}}$ . The fine-tune property of Eq. (5) is similar to that in the low  $\tan \beta$  case. When  $M_{A^0}$  increases, the allowed parameter region by experiments and the  $\sin^2(\beta - \alpha) \leq 0.8$  requirement is minimized, as shown in Fig. 2B.

Third, in the case of large  $\tan \beta = 50$ , since the bottom Yukawa coupling is large compared with the top Yukawa coupling, we concentrate on the contributions of the bottom and sbottom and take  $A_t = 0$  for a while. The experimentally allowed parameter region of  $\mu$  and  $A_b$  is shown in Fig. 3 in both the dotted and star areas, with fixed  $M_{\tilde{q}}$ ,  $M_{\tilde{l}}$ ,  $M_{A^0}$ ,  $A_t$ ,  $M_1$  and  $M_2$ . We notice that  $\mu$  is in a small range near  $1.5M_{\tilde{q}}$  because of the large  $M_b \tan \beta$  in the off-diagonal sbottom mixing term  $M_b(A_b - \mu \tan \beta)$  and  $A_b$  is in the range between  $-9M_{\tilde{q}}$  and  $-10M_{\tilde{q}}$ . The star area is allowed by the requirement of  $\sin^2(\beta - \alpha) \leq 0.8$ . With  $\tan \beta = 50$  and  $\mu \simeq 750\text{GeV}$ , we can see from Eq. (8), the neutralino-smuon loop alone can generate the muon anomalous magnetic moment ( $g - 2$ ) within the experiment bound as shown in Fig. 3A with large  $M_2$ , where

the chargino contribution can be neglected. But because of large  $\tan\beta = 50$  and not too large  $\mu \simeq 750\text{GeV}$ , the chargino-sneutrino loop alone can also generate a value large enough to satisfy the experimental bound, as can be seen from Eq. (7). This case is shown in Fig. 3B, where we choose  $M_1 = 100\text{GeV}$  simply because of the requirement that the neutralino is the LSP. Even in this lower chargino mass case, we need not worry about the  $b \rightarrow s\gamma$  bound, because of nearly degenerate scalar up-type quark masses arising from the assumption of the universal soft supersymmetry breaking squark mass, not too large  $\mu$  and  $A_t = 0$ . When  $A_t \neq 0$ , for example,  $A_t = 150\text{GeV}$ , and the other parameters are the same as those shown in Fig. 3B,  $\text{Br}(b \rightarrow s\gamma)$  reaches its upper bound, because of positive  $\mu A_t$  which leads to that the chargino contribution interferes with that in SM constructively. Furthermore, we can show in our numerical analysis that if we assign a negative value to  $A_t$  (say,  $-500\text{GeV}$ ), the SUSY contributions interfere destructively with that in SM so that the  $b \rightarrow s\gamma$  constraint can be easily satisfied.

The damped  $\sin^2(\beta - \alpha)$  has significant effects on the vertices of  $g_{h^0 W^+ W^-}$ ,  $g_{h^0 Z Z}$  and  $g_{h^0 \gamma \gamma}$  and consequently on Higgs productions at photon colliders, as pointed out in Introduction. With parameters chosen in the regions denoted by the star area in the figures, i. e., the regions allowed by experiments and the requirement of  $\sin^2(\beta - \alpha) \leq 0.8$ , we show our numerical result of the lightest CP-even Higgs production at  $\gamma\gamma$  colliders in Tab. I. Since the dominant contribution to this process comes from  $W^+ W^-$  loop, with damped  $\sin(\beta - \alpha)$ , this  $W^+ W^-$  loop contribution is reduced. For the case C in the table, because  $|\alpha| \sim 0.5$ , the Yukawa coupling of the lightest neutral CP-even Higgs boson to top quarks is lifted from the decoupling case so that the top-antitop loop contribution is also reduced. Therefore, the production cross section is significantly reduced compared with that in SM. In large  $\tan\beta$  limit, the bottom Yukawa effect is enhanced, which corresponds to the case D in which the production section is significantly enhanced compared with that in SM due to  $\alpha \sim -0.5$ . Since the off-diagonal term of the stop mixing matrix is large in the cases A, B and C, as seen in Eqs. (25), (26),  $R_{\tilde{t}}$  enhances the stop contribution significantly. The ratio  $\Delta\sigma_0/\sigma_0^{sm} = (\sigma_0^{MSSM} - \sigma_0^{sm})/\sigma_0^{sm}$  of the lightest Higgs

boson production cross section at photon colliders as a function of  $\mu$  for different  $\tan\beta$  cases are shown in Fig. 1C, 2C, 3C. And additional quantities  $\sin(\beta - \alpha)$ ,  $\sigma_0^{sm}$  and  $M_{h^0}$  are also drawn in Figs. 1,2,3. Fig. 1C is of a clear manifest of the fine-tune property in Eq. (5) with the negative CP-even mixing angle. We can see the ratio  $\Delta\sigma_0/\sigma_0^{sm}$  is significantly different from zero in all three cases of  $\tan\beta$ , with an either decreased or increased change of the lightest Higgs boson production cross section compared with that in SM.

## VI. Conclusions

In summary, through including the radiative corrections to the CP-even neutral Higgs sector from large stop and sbottom off-diagonal matrix elements, we have found allowed parameter regions at small, moderate and large  $\tan\beta$  with damped  $\sin^2(\beta - \alpha)$  of the Higgs couplings and  $M_{A^0}^2 \gg M_Z^2$  under the experimental constraints of lower mass bounds of superparticles and Higgs bosons,  $b \rightarrow s\gamma$  and the recent  $(g - 2)_\mu$ . That is, the decoupling limit is not a necessary consequence of  $M_{A^0}^2 \gg M_Z^2$  and dependent of the other parameters in MSSM, in particular,  $\mu$ ,  $\tan\beta$  and  $A_{t,b}$ , at least in the ranges of values of parameters which we consider in the paper, after one includes the radiative corrections to the Higgs sector. However, with increased  $M_{A^0}$ , the parameter regions are decreased. We find in all three case that there are large deviations of the production cross section of the lightest Higgs boson at photon colliders in MSSM to that in the Standard Model, with either decreased or increased results, which are expected to be tested at the future photon colliders. Finally, one can see from Tab. I that the mass splitting between  $M_H^0$  and  $M_A^0$  is large, which is another implication of non-decoupling limit, as discussed in [19] for the case of the large mass difference between the charged Higgs boson  $H^\pm$  and heavy CP-even Higgs boson  $H^0$ , CP-odd Higgs boson  $A^0$ .

## ACKNOWLEDGMENTS

This research was supported in part by the National Nature Science Foundation of China.

## REFERENCES

- [1] H. E. Haber and G. L. Kane, Phys. Rep. 117(1985)75.
- [2] Y. Okada, M. Yamaguchi and T. Yanagida, Prog. Theor. Phys. 85(1991)1; H. Haber and R. Hempfling, Phys. Rev. Lett. 66(1991)1815; J. Ellis, G. Ridolfi and F. Zwirner, Phys. Lett. B257(1991)83; J. Ellis, G. Ridolfi and F. Zwirner, Phys. Lett. B262(1991)477; R. Barbieri, F. Caravaglios and M. Frigeni, Phys. Lett. B258(1991)167; R. Hempfling and A. Hoang, Phys. Lett. B331(1994)99; J. A. Casas, J. R. Espinosa, M. Quiros and A. Riotto, Nucl. Phys. B436(1995)3; M. Carena, J. R. Espinosa, M. Quiros and C. Wagner, Phys. Lett. B355(1995)209; H. Haber, R. Hempfling and A. Hoang, Z. Phys. C75(1997)539.
- [3] H. E. Haber and Y. Nir, Nucl. Phys. B335(1990)363.
- [4] for a recent review of Higgs, see M. Carena, et al, Report of the Higgs Working Group of the Tevatron Run 2 SUSY/Higgs Workshop, hep-ph/0010338.
- [5] for a review of Photon Collider, see B. Badelek et al, TESLA Technical Design Report, Part VI, Chapter 1: The Photon Collider at TESLA, hep-ex/0108012; D.M. Asner, J.B. Gronberg, and J.F. Gunion, hep-ph/0110320.
- [6] D. L. Borden, D. A. Baner and D. O. Caldwell, Phys. Rev. D48(1993)4018; J. F. Gunion and H. E. Haber, Phys. Rev. D48(1993)5109; M. Kramer, J. H. Huhn, M. L. Stong, P. M. Zerwas, Z. Phys. C64(1994)21.
- [7] T. Ohgaki, T. Takahashi and I. Watanabe, Phys. Rev. D56 (1997)1723; T. Ohgaki, T. Takahashi, I. Watanabe and T. Tauchi, Int. J. Mod. Phys. A13(1998)2411; M. Melles, Nucl. Phys. B(Proc. Suppl.) 82(2000)379; M. Melles, W. J. Stirling and V. A. Khoze, Phys. Rev. D61 (2000) 054015; S. Söldner-Rembold, J. Jikia, hep-ex/0101056; D. M. Asner, J. B. Gronberg, J. F. Gunion, hep-ph/0110320.

- [8] J. Ellis, M. K. Gaillard and D. V. Nanopoulos, Nucl. Phys. B106(1976)292; A. I. Vainshtein, M. Voloshin, V. Zakharov and M. Shifman, Sov. J. Nucl. Phys. 30(1979)711.
- [9] A. Djouadi, V. Driesen, W. Hollik and J. I. Illana, Eur. Phys. J. C1(1998)149; E. Boos et al., hep-ph/0103090 and references therein.
- [10] H. E. Haber, R. Hempfling and A. H. Hoang, Z. Phys. C75(1997),539; M. Carena, S. Mrenna and C. E. M. Wagner, Phys. Rev. D60(1999)075010.
- [11] M. Carena, M. Quiros and C. E. M. Wagner, Nucl. Phys. B461(1996)407; M. Carena, H. E. Haber, S. Heinemeyer, W. Hollik, C. E. M. Wagner, and G. Weiglein, Nucl. Phys. B580(2000)29.
- [12] Muon g-2 Collaboration, H. N. Brown *et al.*, Phys. Rev. Lett. 86 (2001) 2227.
- [13] S. Martin and J. Wells, Phys. Rev. D 64 (2001) 035003, and references therein; M. Byrne, C. Kolda and J. E. Lennon, hep-ph/0108122.
- [14] CLEO Collaboration, S. Ahmed *et al.*, CLEO-CONF-99-10, hep-ex/9908022.
- [15] M. Carena, M. Olechowski, S. Pokorski and C. E. M. Wagner, Nucl. Phys. B426 (1994) 269; M. Carena, D. Garcia, U. Nierste and C. E. M. Wagner, Phys. Lett. B499 (2001)141.
- [16] J. F. Gunion, H. E. Haber, G. L. Kane and S. Dawson, The Higgs Hunter's Guide, Addison-Wesley, 1990.
- [17] R. Hempfling, Phys. Rev. D49(1994)6168; L. Hall, R. Rattazzi and U. Sarid, Phys. Rev. D50(1994)7048; M. Carena, M. Olechowski, S. Pokorski and C. E. M. Wagner, Nucl. Phys. B426(1994)269; D. pierce, J. Bagger, K. Matchev and R. J.Zhang, Nucl. Phys. B491(1997)3.
- [18] Particle Data Group, D. E. Groom *et al.*, Eur. Phys J. C 15 (2000) 1.
- [19] A. G.Akeroyd and S. Baek, hep-ph/0105228.

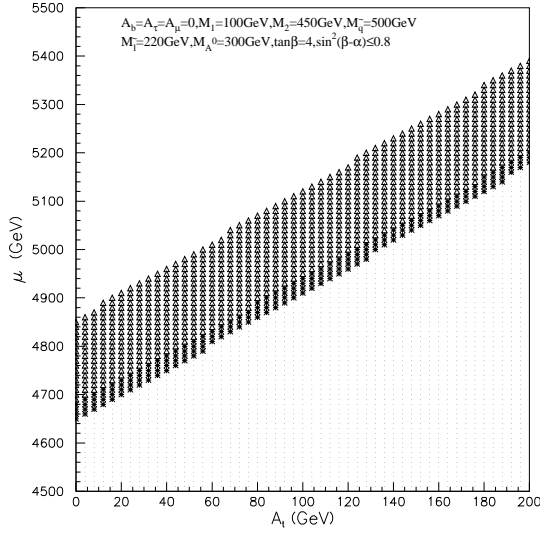
# TABLES

TABLE I. Mss spectra unit (GeV),  $\sigma_0$  in unit fb,  $M_{A^0} = 300\text{GeV}$ ,  $M_1 = 100\text{GeV}$ .

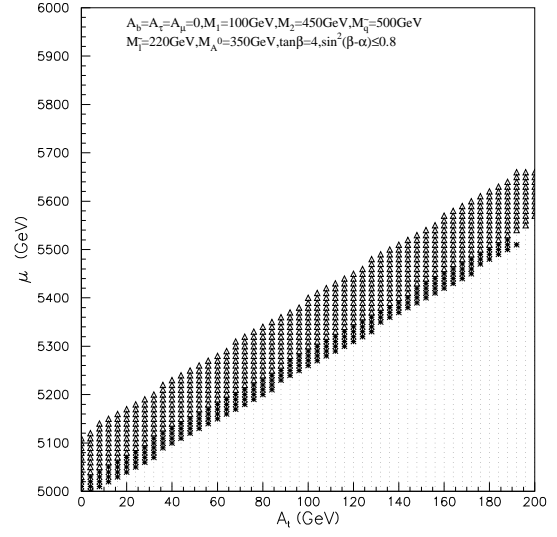
Case	$\tan \beta / M_2 / \mu$	$A_t / A_b$	$M_{\tilde{q}} / M_{\tilde{l}}$	$M_{\tilde{t}_{1,2}}$	$M_{\tilde{b}_{1,2}}$	$M_{\tilde{\tau}_{1,2}}$	$M_{\tilde{\chi}_{1,2}^\pm}$
$M_{\tilde{\chi}_{1,2,3,4}^0}$	$M_{h^0, H^0}$	$(\delta M_{11}^2 / \delta M_{22}^2)$	$(\delta M_{12}^2 / \delta M_{22}^2)$	$\sqrt{\delta M_{22}^2}$	$\alpha$	$\sin(\beta - \alpha)$	$I_W / I_W^{sm}$
$I_t / I_t^{sm}$	$I_b / I_b^{sm}$	$I_{\tilde{t}}$	$I_{\tilde{b}}$	$I_{\tilde{\tau}}$	$\sigma_o$	$(\Delta \sigma_0 / \sigma_0^{sm})$	
A	4/450/4900	72/0	500/220	277/693	411/578	124/291	449/4901
99/449/4900/4901	119/171	-6.6	1.6	98	0.72	0.57	4.7/8.1
-1.4/-1.8	-0.1/0.0	-1.6	-0.0	-0.1	7.7	-0.95	
B	4/450/4800	52/0	500/220	279/692	413/576	126/290	449/4801
99/449/4800/4801	123/178	-6.2	1.5	99	-0.75	0.88	7.3/8.3
-1.4/-1.8	0.1/0.0	1.3	-0.0	-0.1	209.5	0.22	
C	10/450/3200	1750/0	500/270	168/727	342/621	134/363	449/3202
99/449/3200/3201	101/178	-9.8	3.0	80	0.52	0.82	6.3/7.7
-1.6/-1.8	-0.2/0.0	-0.4	-0.0	-0.1	64.0	-0.56	
D	50/1000/760	0/-4800	500/280	525/530	268/657	113/384	748/1015
99/748/762/1015	100/187	-7.2	-1.1	92	-0.55	0.86	6.7/7.7
-1.5/-1.8	0.4/0.0	-0.1	0.0	-0.1	198.7	0.37	



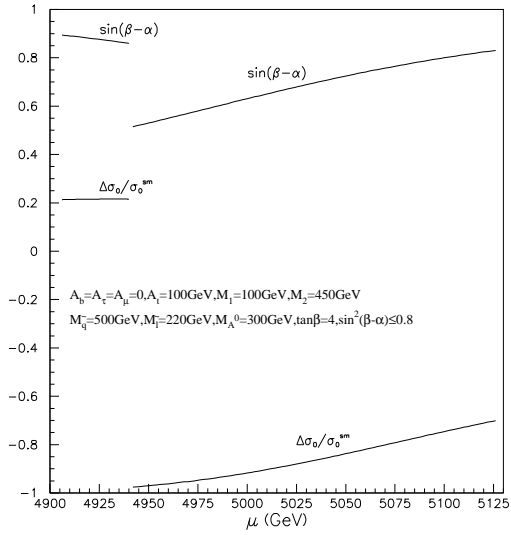
# FIGURES



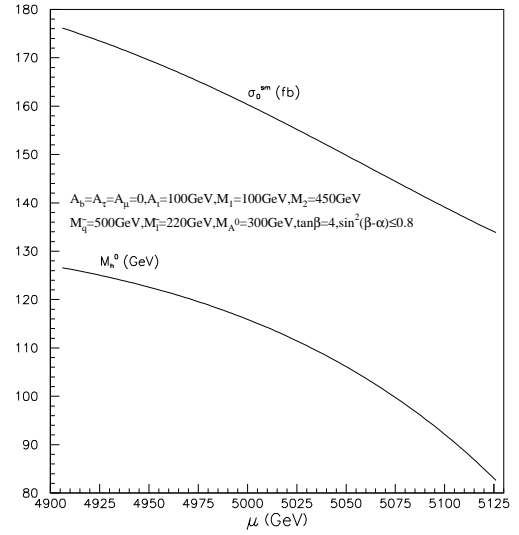
A



B

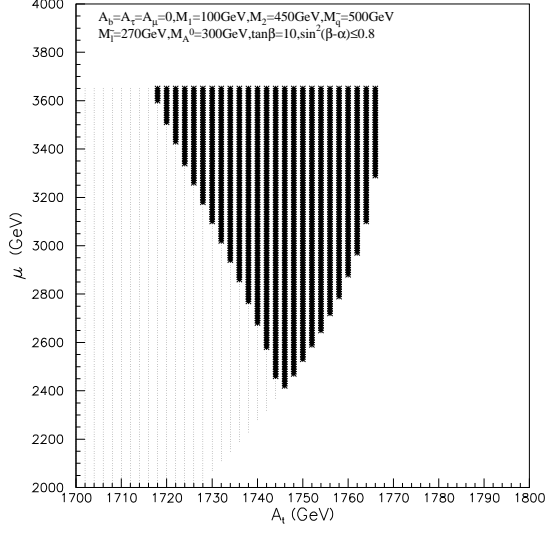


C

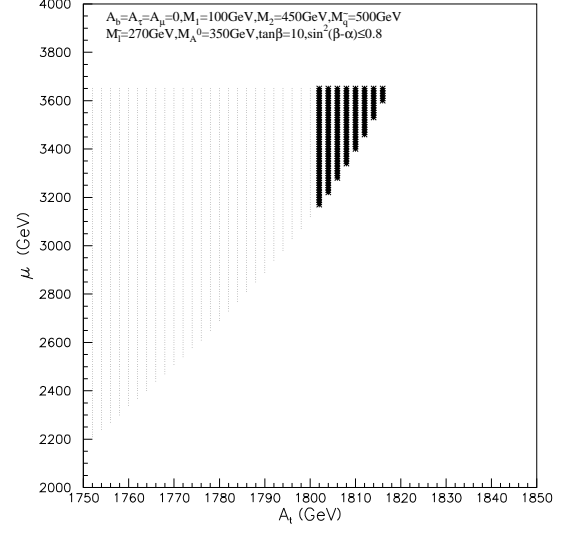


D

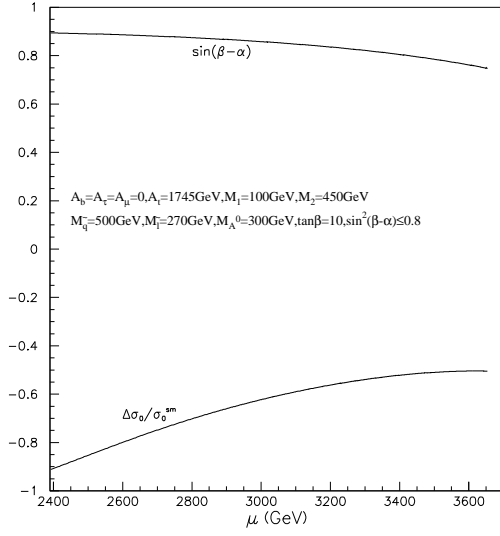
FIG. 1. The low  $\tan \beta = 4$  case. The dotted, triagle and star regions are allowed by experiments. The star (triangle) region corresponds to  $\sin^2(\beta - \alpha) \leq 0.8$  for negative (positive)  $\alpha$ .



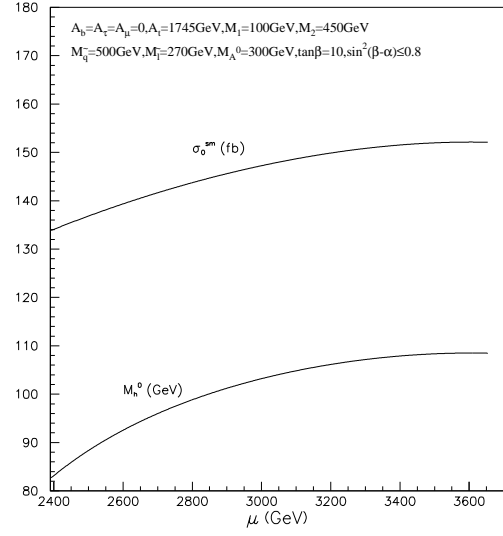
A



B

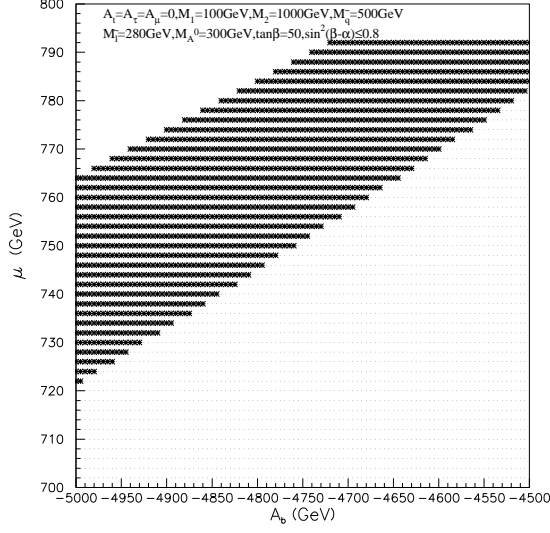


C

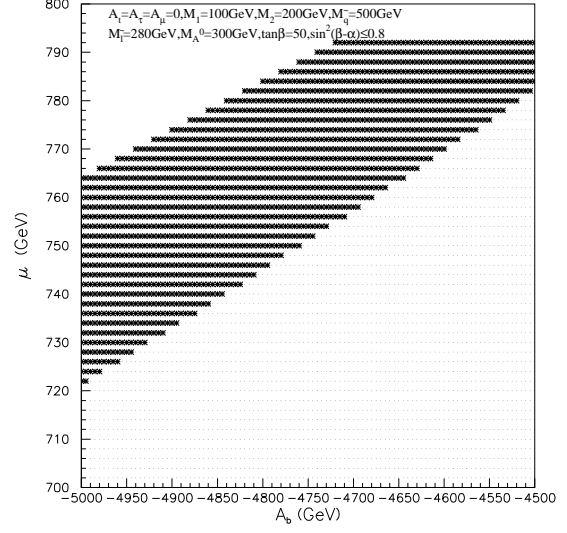


D

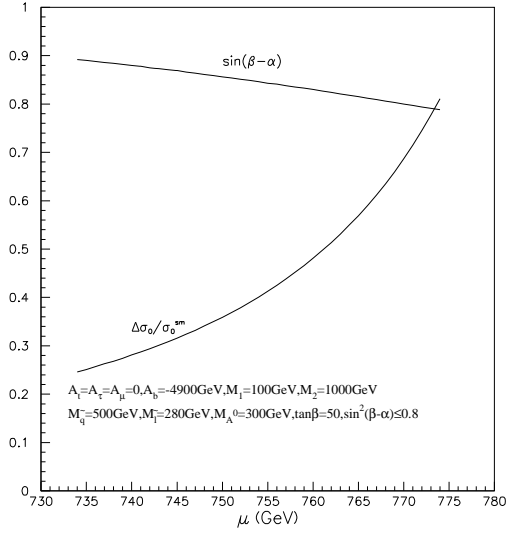
FIG. 2. The moderate  $\tan \beta = 10$  case. The dotted and star regions are allowed by experiments, and the star region corresponds to  $\sin^2(\beta - \alpha) \leq 0.8$ .



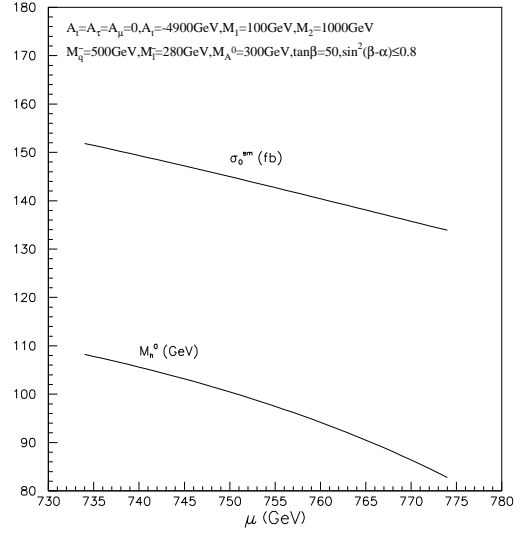
A



B



C



D

FIG. 3. The large  $\tan \beta = 50$  case. The dotted and star regions are allowed by experiments, and the star region corresponds to  $\sin^2(\beta - \alpha) \leq 0.8$ .